Ultrafast dynamics of occupied quantum well states in Pb/Si(111)

2012 New J. Phys. 14 023047

(http://iopscience.iop.org/1367-2630/14/2/023047)

New Journal of Physics
The open-access journal for physics

Ultrafast dynamics of occupied quantum well states in Pb/Si(111)

L Rettig[1,2], **P S Kirchmann**[3] **and U Bovensiepen**[2,4,5]

[1] Fachbereich Physik, Freie Universität Berlin, Arnimallee 14, D-14195 Berlin, Germany
[2] Fakultät für Physik, Universität Duisburg-Essen, Lotharstrasse 1, D-47048 Duisburg, Germany
[3] Abteilung Physikalische Chemie, Fritz-Haber-Institut der MPG, Faradayweg 4-6, D-14195 Berlin, Germany
[4] Zentrum für Nanointegration Duisburg-Essen (CENIDE), Lotharstrasse 1, D-47048 Duisburg, Germany
E-mail: uwe.bovensiepen@uni-due.de

New Journal of Physics **14** (2012) 023047 (17pp)
Received 7 November 2011
Published 21 February 2012
Online at http://www.njp.org/
doi:10.1088/1367-2630/14/2/023047

Abstract. We investigate the ultrafast electron dynamics of occupied quantum well states (QWSs) in Pb/Si(111) with time-resolved photoemission spectroscopy. We find an ultrafast increase in binding energy of the QWSs driven by the optical excitation, while the electronic system is in a non-equilibrium state. We explain this transient energetic stabilization in the photoexcited state by an ultrafast modification of the Fermi level pinning, triggered by charge transfer across the Pb/Si interface. In addition, we observe the excitation of a coherent surface phonon mode at a frequency of ∼2 THz, which modulates the QWS binding energy.

[5] Author to whom any correspondence should be addressed.

Contents

1. Introduction

The structure and energetics of interfaces between semiconductors and metals are of importance from both a fundamental and a technological point of view. In semiconducting devices such as integrated circuits, solar cells or light-emitting diodes, interfaces to metal electrodes play a crucial role in device functionality. Thus, semiconductor surfaces and semiconductor–metal junctions have been intensively studied in a variety of systems [1]. In particular on silicon surfaces, the most commonly used semiconductor for device fabrication, a variety of interface structures and reconstructions with various metal adsorbates have been investigated [1–6]. Already for sub-monolayer (ML) coverages of metal atoms, the occupation of metal-derived surface states within the semiconductor band gap leads to a charge transfer between substrate and adsorbate atoms. This results in a space charge region near the semiconductor interface and the buildup of a Schottky energy barrier [1], which determines the energy band alignment at the interface. However, the ultrafast dynamics describing the response of the energy alignment at the interface to an optical excitation has received only a very little attention so far. First experiments focused on the dynamics of surface photo voltage (SPV) on a slow picosecond to nanosecond timescale [7–9], whereas the femtosecond dynamics directly after excitation remained unexplored.

Time-resolved photoemission (trPES) techniques have been quite successful in investigating the dynamics of excited electrons directly in the time domain. While time-resolved two-photon photoemission is sensitive to unoccupied electronic states and has been used to intensively study the dynamics of hot electron distributions and of surface and image potential states [10–16], time- and angle-resolved direct photoemission analyzes the occupied electronic bands under optical excitation. It has been quite successful in investigating electron dynamics in both simple metals [17, 18] and layered correlated electron materials [19–23], where excitations specific to the ordered nature of the material as well as coherently excited phonons have been observed. However, to investigate the electronic dynamics within the bulk of normal metals, one has to overcome several challenges. Firstly, electronic bands with a strong dispersion perpendicular to the surface, like in many bulk metals, usually show only broad energetic features that limit a comprehensive analysis, due to the finite $k_\perp$ resolution in photoemission spectroscopy caused by the finite photoelectron escape depth. Secondly, electronic transport effects can drastically influence the observed dynamics and can be hard to disentangle from other effects [12, 24, 25]. The use of ultrathin metal films is one approach to overcome these difficulties. The ultrathin metal film breaks the periodicity along the surface normal and the

resulting electron confinement gives rise to sharp quantum well states (QWSs) at discrete energies in the occupied and unoccupied parts of the quantized band structure [26–29]. Owing to their quasi-two-dimensional (2D) character, QWSs show no $k_\perp$ dispersion [28] and their confinement to the ultrathin film effectively inhibits electron transport [29] for electron states with energies within the substrate band gap.

The QWS system of ultrathin epitaxial films of Pb on Si(111) presents a nearly ideal realization of such a quasi-2D model system, which has been intensively studied in the past [29–39]. Owing to the efficient confinement of the electronic wave functions to the metal film by the band gap of the semiconducting substrate, the system exhibits a series of well-defined and sharp QWSs [29, 35–37]. First investigations of the electron dynamics focused on the electron lifetime in unoccupied QWSs [29, 40]. Here, we investigate the ultrafast dynamics of occupied QWSs and states at the Pb/Si interface after photoexcitation. We make use of the selection of Pb coverage and the respective QWS binding energies, as the latter are very sensitive to the energy alignment and the interface structure [6, 38, 39]. Thus, they can serve as a probe for the ultrafast processes at the metal–semiconductor interface. In addition, the laser-based photoemission with low kinetic energies is characterized by an enhanced bulk sensitivity [41], which allows the detection of interface states (ISs) at the buried Pb/Si interface.

We show that the ultrafast modification of the charge balance at the Pb/Si interface after optical excitation leads to an ultrafast change of the Fermi level pinning position and to a transient energy shift of the Si band gap. As a result, the QWS confinement condition is modified and leads to an energetic stabilization of the QWS system. In addition, we observe the excitation of a coherent surface phonon mode which modulates the QWS binding energy.

2. Experimental methods

The experimental setup and procedures have been described in detail elsewhere [35, 40]. The investigated samples of thin epitaxial Pb films were grown *in situ* on Si(111) surfaces under ultrahigh vacuum (UHV) conditions (base pressure $<1 \times 10^{-10}$ mbar). The surface of the silicon wafers was cleaned by repeated flashing to 1470 K, followed by a slow cooling ramp of $-1\,\mathrm{K\,min^{-1}}$ to 970 K to form the Si(111)-7×7 surface reconstruction. The cleanliness of the surface was checked by low-energy electron diffraction. Epitaxial Pb layers were grown on the Si(111)-$\sqrt{3} \times \sqrt{3}$-R30°-Pb reconstruction [35] by evaporation of Pb from a home-built Knudsen cell [35, 36]. The evaporation rate of $\sim$0.5 ML min^{-1} was monitored by a quartz micro balance. Samples were grown in a wedge shape, facilitating measurements of various film thicknesses on a single sample preparation. A shallow thickness gradient of $<0.5\,\mathrm{ML\,mm^{-1}}$ was used to ensure homogeneity of the electronic structure within the measured area [29]. To suppress surface diffusion of Pb atoms and island formation [37], the samples were kept at $T = 80$ K during the experiments.

trPES measurements were carried out using an amplified Ti : sapphire laser system (Coherent RegA 9050) operating at 300 kHz repetition rate. Its fundamental infrared (IR) output at $h\nu_1 = 1.5$ eV is used to optically excite the sample. Alternatively, the output of a tunable optical parametric amplifier (Coherent OPA) in the near-IR or visible range can be used for pumping. The ultraviolet (UV) probe pulses at $h\nu_2 = 6.0$ eV are generated by frequency quadrupling the RegA output by two consecutive β-bariumborate crystals and subsequent recompression by prism pairs. The IR pump pulses have a pulse duration of 55 fs, whereas the UV probe pulse are slightly longer with 80 fs due to nonlinear effects in the quadrupling process.

The cross-correlation (XC) of pump and probe pulses results in an overall time resolution of 100 fs. These time-correlated pairs of femtosecond pump and probe laser pulses, $h\nu_1$ and $h\nu_2$, respectively, are focused into the UHV chamber and spatially overlapped on the sample surface. Typical absorbed pump fluences are of the order of $F = 50$–$1000\,\mu\mathrm{J\,cm^{-2}}$ and below the damage threshold of Pb/Si(111) as no irreversible spectral changes were encountered. The binding energy of the photoemitted electrons is determined from their kinetic energy E_{kin} analyzed in a time-of-flight spectrometer: $E - E_{\mathrm{F}} = E_{\mathrm{kin}} + \Phi - h\nu$. Here, Φ denotes the work function and $h\nu$ the photon energy of the probing laser pulse. The overall energy resolution of typically 50 meV is determined by the spectrometer resolution and the spectral width of the probe pulses. All measurements were carried out in normal emission geometry at the $\overline{\Gamma}$-point with an angular resolution determined by the spectrometer acceptance angle of $\pm 3.5^{\circ}$.

The metal–semiconductor interface between the Si substrate and the Pb film leads to a charge transfer between substrate and metal film, as the Fermi level E_{F} is pinned by localized charges at the interface, the so-called metal-induced gap states (MIGS) [1]. This results in a space charge region of typically several 100 nm thickness within the Si substrate and leads to band bending near the surface depending on the doping level as sketched in figure 1(b) for a p-doped substrate. Photo-generated electron–hole pairs are separated in the space charge region and lead to a reduction in the band bending, see figure 1(c). This results in a potential difference between interface and bulk, known as surface photo voltage (SPV) [1].

The SPV manifests in a photoemission experiment as a rigid shift of the spectra, as the energy reference of the spectrometer is determined by the bulk Fermi level. Figure 1(a) shows photoemission spectra of 5 ML Pb/Si(111) with and without excitation by the pump pulse arriving after the probe pulse, i.e. at negative pump–probe delays. The details of the spectra will be discussed below. On a p-Si substrate, the spectrum is—in comparison to a reference spectrum taken without optical excitation (black/solid line)—rigidly shifted to higher kinetic energy (blue/large dashed line), including the secondary cutoff at low kinetic energies, which is determined by the sample work function. In contrast, on an n-Si substrate, the spectrum is shifted toward lower kinetic energy. This is well understood from the opposite orientation of the space charge field for n- and p-doped semiconductors, leading to a reversed charge separation. Additionally, the shift on an n-Si substrate is considerably larger. The amount of the SPV has been determined for various fluences for both n- and p-Si, as shown in figure 1(d). We note that (i) the SPV saturates for fluences $F > 50\,\mu\mathrm{J\,cm^{-2}}$ and (ii) is considerably weaker on p-Si. Thus, the usage of p-Si substrates and excitation fluences $F > 50\,\mu\mathrm{J\,cm^{-2}}$, as used for all time-resolved measurements, minimizes the effect of the SPV and ensures flat-band conditions as shown in figure 1(c). Since the dynamics of the SPV happens on a nanosecond timescale [7], it can be considered as constant within the time interval of a few picoseconds after excitation investigated here[6]. An SPV induced by the probe beam is negligible as was checked by the variation of the probe fluence.

3. Results and discussion

In the following, we will discuss the modifications of the occupied electron states that occur on an ultrafast timescale and are driven by the photoexcitation. Here, we will discuss two main

[6] Although the SPV is built up by the pump pulse, the shift of trPES spectra is also found for negative delays close to time zero as explained in [7].

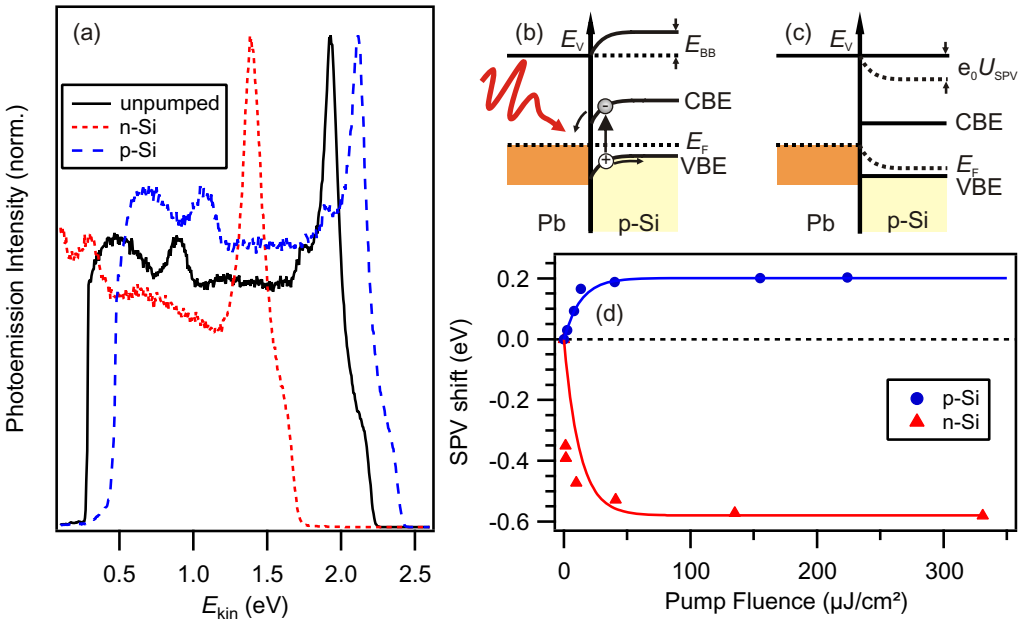

Figure 1. (a) Effect of SPV on the photoemission spectra of 5 ML Pb/Si(111). The black (solid) line shows a reference spectrum without the pump beam. Red (small dashed) and blue (large dashed) spectra are taken with a pump fluence of $F = 40\,\mu\mathrm{J\,cm^{-2}}$ on n-Si and p-Si substrates, respectively. Owing to the SPV, the whole spectra are shifted in kinetic energy. (b) The Schottky junction in equilibrium. The Fermi level pinning at the interface leads to a space charge region and to band bending E_{BB}. The conduction band edge (CBE), valence band edge (VBE) and vacuum level (E_{V}) are indicated. An incident photon with an energy above the band gap excites electron–hole pairs across the band gap, which are separated in the space charge region. (c) The Schottky junction after optical excitation. The SPV reduces the band bending, leading to flat bands for high enough excitation densities. The Fermi level at the interface is shifted by the SPV. (d) Measured SPV shift as a function of pump fluence for p-Si (blue circles) and n-Si (red triangles) substrates, respectively. Lines are a guide to the eyes.

features: First, we will use moderate excitation densities and focus on a transient increase in binding energy that builds up on an ultrafast timescale within the time resolution of the experiment. In the second part, we analyze a periodic modulation of the QWS binding energy that is superimposed on the continuous shift and is attributed to the excitation of a coherent surface phonon mode.

3.1. Transient binding energy shift

Let us now turn to the spectral features and their modification with optical excitation. Figure 2(a) shows spectra of a 5 ML Pb film on Si(111) with a moderate excitation fluence of $F = 60\,\mu\mathrm{J\,cm^{-2}}$ before (filled black symbols) and 100 fs after excitation (open red symbols). Besides the high-energy cutoff at the Fermi energy and the sharp low-energy cutoff (secondary

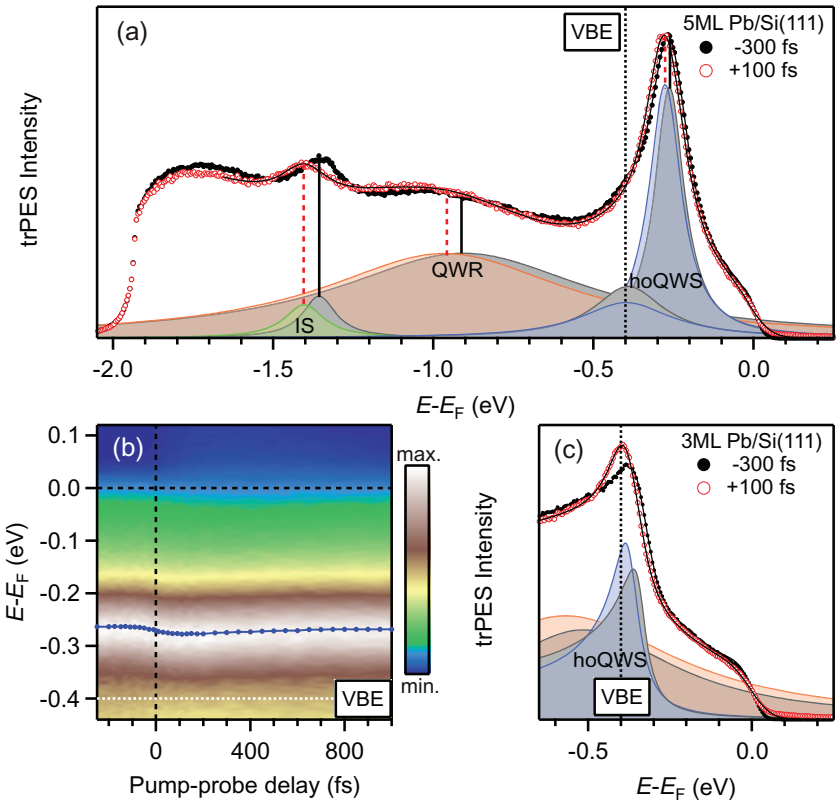

Figure 2. (a) trPES spectra of a 5 ML Pb film before (black filled circles) and 100 fs after optical excitation (red open circles). Solid lines are fits to the data (see the text). The pronounced peak at $E - E_F = -0.26$ eV is the highest occupied quantum well state (hoQWS). In addition, a broad quantum well resonance (QWR) and an IS at the Pb/Si interface are observed. The peaks used in the fitting model are shown as shaded areas and the peak positions as determined by the fits are indicated, exhibiting a peak shift ΔE to higher binding energy. The small shoulder at $E - E_F \sim -0.4$ eV is the hoQWS of small areas with 3 ML coverage within the probed spot. (b) trPES intensity for 5 ML coverage in a false color plot as a function of pump–probe delay. The blue line and symbols mark the peak position of the hoQWS obtained by fitting the spectra (see the text). (c) trPES spectra as in (a), but for 3 ML Pb/Si. Note the pronounced asymmetry of the hoQWS line shape near the silicon VBE, which is reduced upon excitation.

edge) at $E - E_F = -1.9$ eV, determined by the sample work function of $\Phi = 4.1$ eV, we find three main features in the spectrum. The most prominent peak at $E - E_F = -0.26$ eV is the hoQWS, which resides well above the silicon VBE at $E - E_F \sim -0.4$ eV. Its sharpness and high intensity evidence the strong confinement to the Pb surface layer, in agreement with earlier photoemission work [29, 37, 40]. In contrast, the broad QWR at $E - E_F = -0.94$ eV lies within the Si valence band and is degenerate with bulk Si valence band states. The third feature at $E - E_F = -1.39$ eV is assigned to an IS at the Pb/Si interface, as it appears at all coverages at roughly the same energy and does not show the characteristic energy dispersion of the QWSs in Pb/Si(111) [30, 40]. Moreover, this state is also present on the bare Si(111)-$\sqrt{3} \times \sqrt{3}$-R30°-Pb

surface and is less pronounced for higher Pb coverages, as photoemitted electrons from the interface have to traverse a thicker Pb film before emission into the vacuum.

Upon photoexcitation, all states exhibit an energy shift ΔE to higher binding energies, as recognized from the solid and dashed lines in figure 2(a), which mark the peak position before and after the laser excitation, respectively. This shift is rather small for the hoQWS, whereas it is considerably larger for the QWR and the IS. Quantum well states near the Si VBE, such as the hoQWS of a 3 ML film shown in figure 2(c), are characterized by a pronounced asymmetry of the line shape, indicating the transition from QWSs to QWRs, as the confinement weakens in the vicinity of the VBE. Upon excitation, however, in addition to the peak shift, this asymmetry is considerably reduced. As will be discussed in the following, this change in the line shape indicates a transient enhancement of the electronic confinement conditions of the QWSs.

At this point, we note that the shift in binding energy is qualitatively different from the energy shift induced by the SPV effect. The SPV leads to a shift of the whole spectrum, including the Fermi and the secondary edge (see figure 1) and does not change the peak position relative to the Fermi level. This is in contrast to the shift in binding energy after photoexcitation, which affects only the peak positions relative to the secondary edge and E_F. This is apparent from the secondary edge and the Fermi cutoff in figure 2(a), which do not shift. Furthermore, the effect of the SPV is constant in the time window discussed here, and its direction depends on the doping level of the substrate. In contrast, the peak shift in figure 2 occurs in the same direction both on p- and n-doped Si samples (not shown).

The dynamics of the peak shift is analyzed in a false color representation of the trPES intensity as a function of the pump–probe delay, shown in figure 2(b). The peak position of the hoQWS, indicated by the blue markers, shows that the peak shift occurs on a very short timescale of ∼100 fs after excitation, followed by a slower relaxation toward the initial peak position. For a more quantitative analysis, the relative peak shift ΔE is determined by fitting the trPES spectra with a series of Lorentzian lines and an exponential background function, multiplied with a Fermi–Dirac distribution and convoluted with an instrument function. The fits and the contributing peak functions are shown as thin black lines and shaded areas, respectively, in figures 2(a) and (c). For the hoQWS of 3 ML Pb/Si (figure 2(c)) a Doniach–Šunjić line shape [42] has been used in order to account for the pronounced peak asymmetry. The fit yields a Doniach–Šunjić asymmetry parameter α of 0.51(1), which decreases significantly to 0.35(1) after photoexcitation, see figure 2(c).

The resulting peak shifts are shown in figure 3(a) for the three states in figure 2(a) as a function of pump–probe delay. For comparison, figure 3(b) shows the pump–probe pulse XC, determining the temporal resolution of the experiment and the temporal overlap of pump and probe pulses (time zero, t_0). To determine the maximal peak shift ΔE_{max} and the timescale of its recovery τ, exponential decay functions, $\Delta E(t) = -\Delta E_{max} \exp(-t/\tau) + B$, convoluted with the pump–probe envelope, are fitted to the data. Here, B accounts for a transient equilibrium after relaxation of the initial dynamics. For the hoQWS, we find a small maximal peak shift of $\Delta E_{max}^{hoQWS} = 17(2)$ meV. In contrast, the QWR and the IS show a much stronger peak shift of $\Delta E_{max}^{QWR} = 66(6)$ meV and $\Delta E_{max}^{IS} = 52(4)$ meV, respectively. The relaxation times of all three states are found to be about 500 fs ($\tau_{hoQWS} = 460(90)$ fs, $\tau_{QWR} = 610(150)$ fs and $\tau_{IS} = 600(90)$ fs).

The comparison of the peak shift transients with the pulse XC reveals that the initial buildup of the peak shift occurs within the time resolution of our experiment. We consider this ultrafast timescale as evidence for the electronic origin of the responsible processes, as

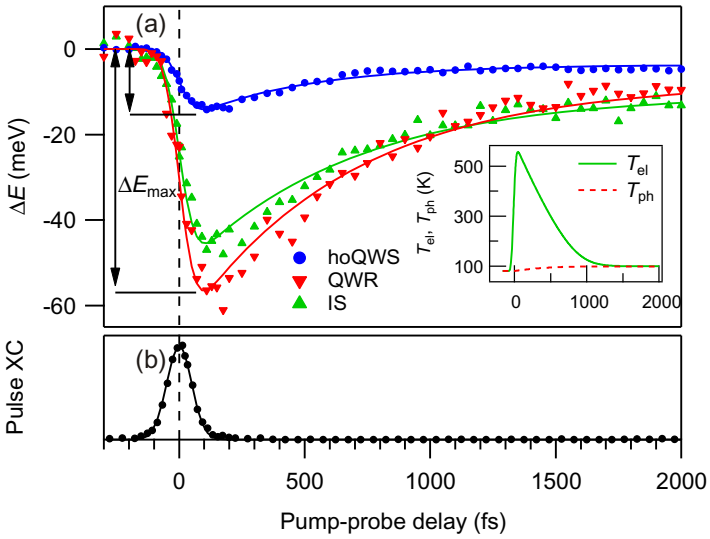

Figure 3. (a) Peak shift ΔE of the three states shown in figure 2(a) as a function of pump–probe delay. Solid lines are exponential fits to the data (see the text). The buildup of the peak shift occurs for all three peaks within the pulse duration of ∼100 fs. The maximal peak shift ΔE_{max} is reached for all peaks at ∼100 fs, followed by a relaxation toward a transient equilibrium. The inset shows the transient electron and lattice temperatures, T_{el} and T_{ph}, respectively, obtained from a two-temperature model (2TM) simulation (see the text). (b) XC trace of the two laser pulses obtained from excited electrons at $E - E_{\mathrm{F}} > 1.4$ eV.

electron–hole pairs are initially excited by the laser pulse. The energy transfer to the lattice occurs at later times and thus effects related with lattice dynamics are typically limited to slower timescales in metals. Electron thermalization and electron–lattice equilibration has been intensively studied in metallic systems [18, 43] and can be described phenomenologically in the context of the 2TM [18, 44–47]. This model treats the electronic and phononic subsystems as two coupled heat baths with electronic temperature T_{el} and lattice (phononic) temperature T_{ph}, respectively. Although this model bears several limitations and simplifications, e.g. the assumption of a constant density of states or a thermalized electron system, model calculations of the 2TM can be used to estimate the electron–lattice equilibration time in Pb/Si, as shown in the inset of figure 3(a). In the calculation, electronic diffusion and transport processes have been neglected to account for the confinement to the ultrathin metal film and the experimental excitation conditions have been used. The calculated electronic temperature T_{el} shows a steep rise at t_0 and a relaxation within 1 ps, comparable to the relaxation of the peak shift. In contrast, the lattice temperature T_{ph} increases only slightly after several 100 fs, further supporting the electronic origin of the peak shift.

In order to compare the peak shifts found on different coverages of Pb/Si(111), the maximal peak shift ΔE_{max} of interface and quantum well states is plotted in figure 4 for various film thicknesses as a function of the respective equilibrium peak position. We find a pronounced dependence of ΔE_{max} from the peak position relative to the Si VBE: below the VBE, for QWRs and the ISs, we find a comparably strong shift of ∼60 meV, which does not depend within our accuracy on the energetic position. Above the VBE, however, for QWSs which are well confined

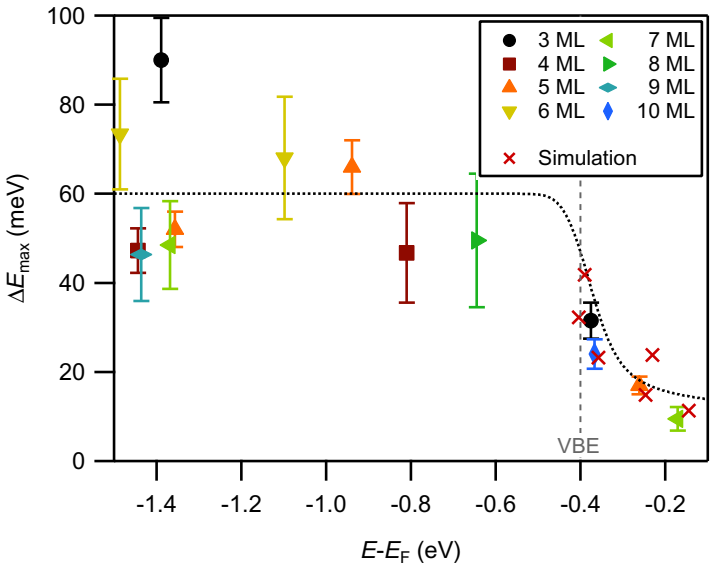

Figure 4. Maximal peak shift $\Delta E_{\max}$ of interface and quantum well states as a function of peak position for various film thicknesses. Red crosses mark the results of a model calculation of the phase accumulation model (see the text). The dashed line is a guide to the eyes. Note the strong reduction of $\Delta E_{\max}$ for QWSs confined above the silicon VBE.

to the Pb film, the peak shift decreases to only ∼10 meV at energies above −0.2 eV. This clear correlation of the size of the peak shift with the peak position relative to the Si valence band which we establish here indicates its relation to the silicon band gap. Furthermore, as already mentioned before in the context of figure 2(c), states close to the VBE exhibit in addition to the peak shift a sharper and more symmetric line shape upon excitation, which we explain as a transient increase in confinement of the QWSs to the Pb film. This corresponds to a transient shift of the Si band gap relative to the metal substrate's Fermi level, i.e. a modification of the Fermi level pinning position at the interface.

In order to determine the amount of band gap shift, we recall that the ISs at higher binding energies are located at the Pb/Si interface and are derived from Si states. Thus, these states are fixed to the energy reference of the Si substrate, i.e. the position of the Si band edges. Hence, we can use the peak shift of the ISs as a marker for the transient band gap shift, which, in turn, leads to a change of the confinement and a shift of the QWS binding energy.

To test this hypothesis, we have performed a simulation in the framework of the phase accumulation model [28, 37, 48]. The energy position of a QWS is determined by the confined wave function along the metal film's normal direction. In this model, electrons propagating between the Pb/Si interface and the Pb surface are reflected at each interface, exhibiting a phase shift Φ_i and Φ_s, respectively. According to the Bohr–Sommerfeld quantization rule, the total phase accumulated during a round trip, Φ, has to equal a multiple of 2π for a stationary state:

$$\Phi = 2kd + \Phi_i + \Phi_s = n \cdot 2\pi. \tag{1}$$

Here, k is the electron wave number, d the film thickness and n an integer number. This condition determines the allowed electron wave vectors and hence the energetic positions of the QWSs.

The phase factors Φ_i and Φ_s are energy dependent and two approximations are commonly used for these expressions. The surface potential is usually described by the image potential, leading to a phase shift of [28]

$$\Phi_s = \pi \left(\left[\frac{3.4}{E_V - E} \right]^{1/2} - 1 \right), \tag{2}$$

where E_V is the vacuum energy level. For modeling of the phase shift Φ_i at the Si/Pb interface, an empirical formula for the phase shift of π across a band gap in a two-band model is used [37, 48, 49]:

$$\Phi_i = \mathrm{Re}\left[-\arccos\left(2\frac{E - E_{VBM}}{E_G} - 1 \right) \right] + \Phi_0 , \tag{3}$$

with the valence band maximum E_{VBM} and the size of the band gap E_G. Φ_0 denotes a phase offset used as a fit parameter to adjust the model to the data. Despite the simplicity of the model, we achieve reasonable agreement with the energy positions of the QWSs within the band gap [29] and reproduce the characteristic 2 ML periodicity of the dispersion of QWS binding energies with thickness [30].

The effect of a photo-induced band gap shift on the QWS energies was determined by shifting the band edge in the model by $\Delta E_{VBM} = -60$ meV, the value that we determined from the ISs in the experiment. The resulting shift in QWS binding energy is plotted as red crosses in figure 4. We find close agreement with the experimentally determined peak shifts, which increase strongly toward the Si VBE, as indicated by the dashed line. Within the model, this is understood by the increasing slope of the arccos function near the band edge in equation (3), which results in a stronger response to the shift in the band gap at these energies.

Now we discuss possible origins of the transient band gap shift at the interface. Since this shift occurs in the same direction on n- and p-doped silicon samples, we can exclude a direct influence of the space charge layer, as this is inversed in n-doped silicon and would lead to a reversed effect. Furthermore, the effect is also present for excitation wavelengths below the Si bulk band gap (not shown), where no excitation within the silicon substrate is possible by a one-photon absorption process. Thus, the shift of the band gap must be due to changes happening at the interface or within the Pb overlayer. Since the pinning position of the Fermi level at the interface is directly determined by the charge transfer at the interface and the population of MIGS, a modification of this charge balance upon excitation is the most likely origin of the observed effect.

Still, the direction of the peak shift toward *higher* binding energy is intriguing. A usual expectation would be that additional energy delivered by the optical excitation leads to a destabilization of the system, i.e. a softening of the electronic bonds and a decrease of binding energies. Here, however, we find an energetic *stabilization* upon photoexcitation, contrary to this expectation. From the experimentally observed increase in binding energy, we conclude that the strong perturbation by the optical excitation leads to a transient depopulation of MIGS and an electron transfer from the film to the bulk, as sketched in figure 5. This results in a stronger band bending on p-Si, as more bulk acceptors become negatively charged, and a downshift of the band gap relative to the Fermi level on an ultrafast timescale. In n-Si, the charge transfer leads to a reduction of the band bending, as additional bulk donors are neutralized. The IS located at the Pb/Si interface is shifted along with the band gap. In turn, the shifted band gap results in a change in the confinement condition for the QWSs in the

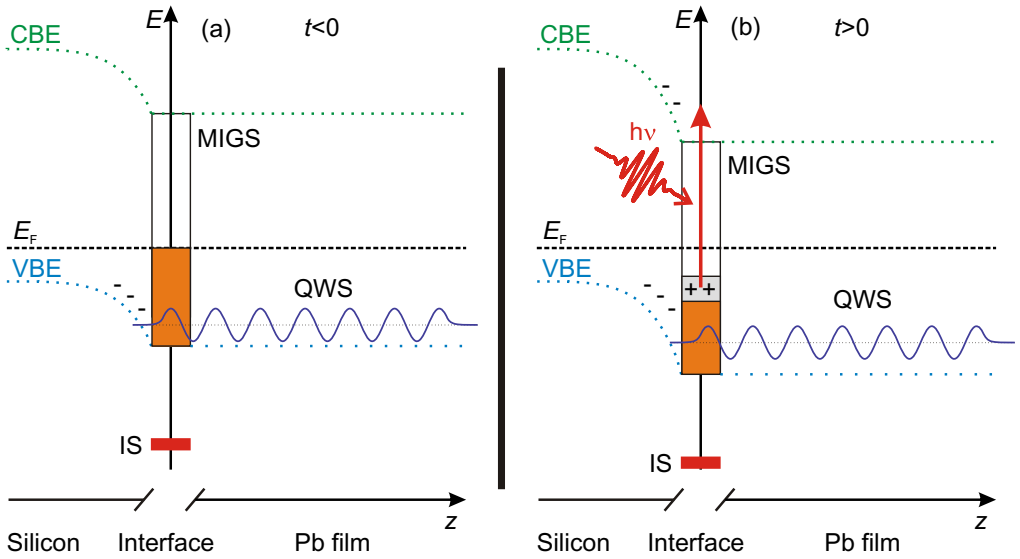

Figure 5. Schematic energy diagram near the Pb/Si interface. (a) Before excitation, the MIGS at the interface are populated to a certain level, pinning the Fermi level E_F. This leads to band bending and a space charge region within the substrate, as sketched for p-type doping. VBE and CBE are indicated by dashed green and blue lines, respectively. (b) Photoexcitation leads to a depopulation of MIGS and a charge transfer toward the bulk. This increases the band bending and shifts the band gap to lower energies. The IS is shifted by the same amount. Owing to the modified confinement conditions by the shifted band gap, the QWS binding energies are likewise shifted away from E_F.

metal film, which leads to a shift of their binding energies. Simultaneously, states near the band edge, which are only weakly confined before excitation and show asymmetric peak shapes, become more symmetric after excitation due to the enhanced confinement by the shifted band edge.

3.2. Coherent phonon excitation

In addition to the incoherent peak shift induced by the transient modification of the confinement condition, we find a coherent response of the system to the optical excitation if we increase the excitation by a factor of 20. Figure 6(a) depicts the transient trPES intensity of 5 ML Pb/Si with an absorbed fluence of $F = 1.1\,\mathrm{mJ\,cm^{-2}}$ in a false color map. The larger shift of the hoQWS ($\Delta E_{\max} = 41(4)$ meV) and the depletion of the intensity at $E - E_F < -0.4$ eV evidence the stronger excitation of the system. The gray contour lines highlight the population of unoccupied states induced by the strong optical excitation. From the spectral weight in the excited state spectrum we estimate an excitation level of >9% of the valence electrons in a window of 1 eV around E_F. The distinct unoccupied state at $E - E_F = 1.1$ eV visible through the closed contour line around zero pump–probe delay is identified as the lowest unoccupied QWS [29]. The excess energy in the electronic system relaxes on a timescale up to 3 ps through electron–phonon coupling and is transferred to the phononic system, leading to substantial lattice heating at these excitation densities. This results in a thermal expansion of the Pb film and induces an additional

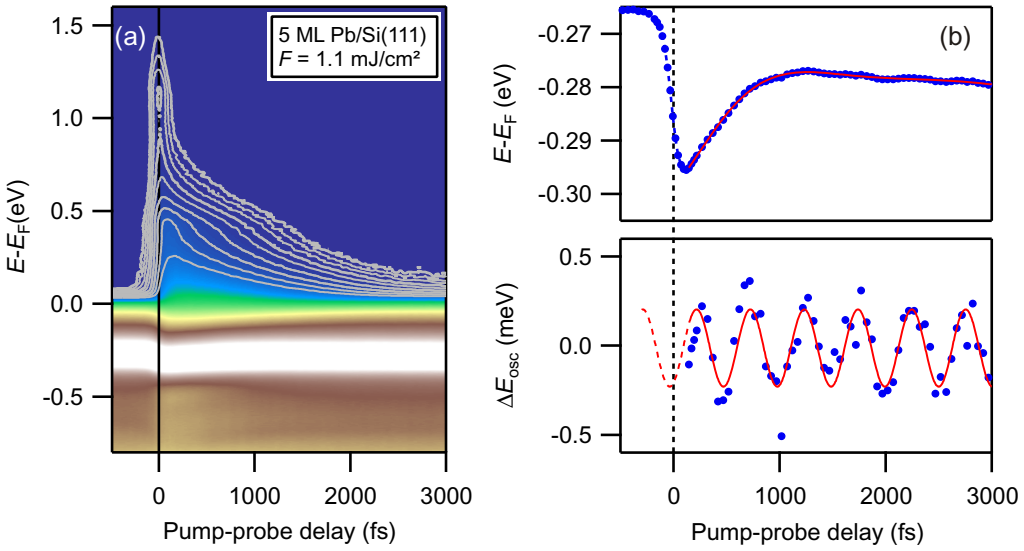

Figure 6. (a) Photoemission intensity as function of $E - E_F$ and pump–probe delay for 5 ML Pb/Si(111) using an absorbed excitation fluence of $F = 1.1\,\mathrm{mJ\,cm^{-2}}$. Note the large number of excited carriers above the Fermi level, highlighted by the contour lines. The state visible at $E - E_F = 1.1\,\mathrm{eV}$ (closed contour lines) is the lowest unoccupied QWS [29]. (b) Upper panel: peak position of the hoQWS determined from a fit as a function of pump–probe delay, showing a transient coherent modulation after excitation. The red line is a fit to extract the incoherent contribution. Lower panel: relative peak shift after subtracting the incoherent contribution, highlighting the coherent oscillations. The red line is a sine fit to the data.

slow shift of the binding energy after the recovery of the initial peak shift at $t > 1$ ps in figure 6, which was not observed at lower excitation densities (figure 3) and persists up to 3 ps.

The transient binding energy of hoQWS as determined by fitting the peak position is depicted in figure 6(b) together with a polynomial background function. On top of the pronounced shift of the peak position which was discussed in the previous section, we see a weak periodic modulation of the peak position with a period of ∼500 fs. To analyze the oscillating contribution to the peak shift, the incoherent background determined by the polynomial fit is subtracted, yielding the coherent oscillatory part of the peak shift, ΔE_{osc}, which is shown in the lower panel of figure 6(b). Remarkably, the high dynamic range in trPES intensity of $>10^5 : 1$ combined with the systematic analysis of fitting the peak position enables the observation of very small relative energy variations of only ∼1 meV, which is significantly below the experimental energy resolution of 50 meV. A fit of a sine function to the data, shown as a thin red line, yields a frequency of $\nu = 1.97(6)$ THz and an initial oscillation phase of $\phi = 0.4(2)\,\pi$, as indicated by the dashed extrapolation of the fit to zero pump–probe delay. A fast Fourier transform of ΔE_{osc} exhibits a sharp peak at a frequency of 2.0(1) THz that corroborates the results of the sine fit.

This brings up the question of the origin of the binding energy oscillation. The frequency of the oscillations of a few THz is in the range of acoustic or low-energy optical phonon modes of typical metals. Indeed, the optical excitation of coherent lattice vibrations by fs laser pulses is a

rather common phenomenon and has been intensively studied in various materials [50–53]. One prerequisite for this process is the existence of phonon modes with finite energy at the Brillouin zone (BZ) center ($q = 0$), typically optical phonon modes, because the optical excitation does not provide a finite momentum. However, the face-centered cubic unit cell of Pb supports only acoustic phonon branches with vanishing energy at the BZ center. The phonon spectrum of Pb shows a pronounced peak around 2 THz [54, 55] and the highest-energy modes around 2.1 THz are found in the longitudinal phonon branch near the BZ boundary along the Γ–L direction [56], which is perpendicular to the film direction. To provide the momentum necessary for optical excitation of such modes, the broken symmetry perpendicular to the film has to be considered, giving rise to new phonon modes at the BZ center. More recent calculations of lattice dynamics in freestanding Pb slabs by Yndurain *et al* [57] predicted longitudinal surface phonon modes at the BZ center with frequencies around 2 THz that show an oscillatory behavior of the phonon frequency with varying slab thickness and describe oscillations of the topmost atomic layers perpendicular to the surface [57]. The existence of such surface phonon modes with frequencies around 2.1 THz at $q = 0$ has been experimentally confirmed by He atom scattering on thin Pb films grown on Cu(111) [58]. Thus, we consider the coherent excitation of a surface phonon mode as the origin of the periodic binding energy modulations.

Still, typical materials exhibiting coherent phonon excitations are semiconductors, semimetals or rare earth metals such as Tb and Gd [59]. In simple s–p metals such as Pb, coherent phonon excitation has not been observed so far. A reason for this could be the efficient screening of excited carriers, resulting in a low excitation probability. Furthermore, the usually considered excitation of coherent phonons by inelastic stimulated Raman scattering requires a resonant interband transition at the pump photon energy [51], which was not directly observed here.

At surfaces, an ultrafast charge separation has been discussed as the driving force for the excitation of coherent surface vibrations [60]. Such a charge separation could be mediated in the Pb/Si quantum well system as discussed in the following. The ultrafast excitation of a comparably large fraction of the valence electrons leads to a spatial redistribution of the electrons at the surface. This is a result of the vacuum potential, which presents a lower vacuum barrier for excited electrons at higher energies. Hence, their wave functions have a smaller damping outside the metal surface, leading to a larger electron density outside the film, the so-called electron spill-out. This leads to an electron dipole at the surface, which was already observed earlier in the modulation of the work function of Pb/Si(111) with Pb coverage due to the changing electron density near the Fermi level [35]. This ultrafast modification of the surface dipole induces a driving force on the surface atoms perpendicular to the surface, leading to the excitation of a coherent surface phonon mode.

This brings up the question of how the surface phonon mode modifies the binding energies of QWSs within the metal film. This can be understood from the strong sensitivity of the QWS binding energies to the width of the quantum well, i.e. the film thickness. If we consider the modification of the film thickness due to an oscillating topmost atomic layer, we can estimate the oscillation amplitude in real space from the phase accumulation model. From the amplitude of the coherent binding energy modulation of ∼1 meV we found in the experiment, we estimate for the 5 ML film that already a modification of ∼2‰ of the interlayer distance, i.e. $<10^{-2}$ Å, leads to the observed binding energy oscillation. This demonstrates that the high sensitivity of QWS binding energies to the film thickness provides a sensitive tool to study very small lattice dynamics in a well-defined low-dimensional system.

4. Conclusion and outlook

In summary, we have investigated the ultrafast electron dynamics in the quantum well system Pb/Si(111) after intense optical excitation using trPES spectroscopy. We find a transient shift of the binding energies of interface and quantum well states to higher binding energies, i.e. an energetic stabilization, which occurs within the time resolution of our experiment. This peak shift is found to be independent of substrate doping and excitation wavelength relative to the band gap, demonstrating an effect located at the interface between Si substrate and metal film. By analyzing the peak shift for various film thicknesses and QWSs at different positions relative to the substrate band gap, we identify a transient ultrafast shift of the band gap relative to the metal Fermi level as the origin of the peak shift, mediated by a photo-induced charge depletion of MIGS. This scenario is corroborated by a simulation within a phase accumulation model.

Thereby our experiments demonstrate an ultrafast modification of the Fermi level pinning position and hence the Schottky barrier height, which is a technologically important property for metal–semiconductor interfaces. Ultimately, this might lead the way toward electro-optical switching devices, at the interface of optical and electronic circuitry. Furthermore, the transient modification of the confinement condition of QWSs and the resulting influence on the QWS line shape and position demonstrate in a descriptive manner the influence of the quantum confinement on QWS wave functions in a prototypical quantum system. Therefore, it would be instructive to investigate QWSs on different substrates, e.g. QWSs in Pb/Cu(111) [16, 61] or Pb/SiC [62] or with different interface structures [36, 39] in future experiments.

Using a much stronger excitation fluence of $F > 1\,\mathrm{mJ\,cm^{-2}}$, we observe in addition to this continuous shift a periodic modulation of the binding energy with a frequency of $\nu = 1.97(6)\,\mathrm{THz}$. We attribute this oscillation to a coherently excited phonon mode at the surface of the Pb film, to our knowledge the first observation of a coherent phonon in a simple s–p band metal. We suggest the coherent excitation of such surface vibrations through the ultrafast redistribution of carriers at the surface. The oscillation of the surface phonon's frequency with the film thickness predicted by Yndurain *et al* [57] encourages further systematic thickness-dependent investigations.

Acknowledgments

This work has been supported by the Deutsche Forschungemeinschaft through BO 1823/2 and SFB 616. The authors acknowledge stimulating discussions with M Weinelt. PSK gratefully acknowledges support from the International Max–Planck Research School 'Complex Surfaces in Material Science' and the Alexander von Humboldt Foundation via a Lynen Stipend.

References

[1] Moench W 1993 *Semiconductor Surfaces and Interfaces* (Berlin: Springer)
[2] Carlisle J A, Miller T and Chiang T-C 1992 Photoemission study of the growth, desorption, Schottky-barrier formation, and atomic structure of Pb on Si(111) *Phys. Rev.* B **45** 3400
[3] Heslinga D R, Weitering H H, van der Werf D P, Klapwijk T M and Hibma T 1990 Atomic-structure-dependent Schottky barrier at epitaxial Pb/Si(111) interfaces *Phys. Rev. Lett.* **64** 1589
[4] Hupalo M, Schmalian J and Tringides M C 2003 'Devil's staircase' in Pb/Si(111) ordered phases *Phys. Rev. Lett.* **90** 216106

[5] Zhang Z, Niu Q and Shih C-K 1998 'Electronic growth' of metallic overlayers on semiconductor substrates *Phys. Rev. Lett.* **80** 5381
[6] Ricci D A, Miller T and Chiang T-C 2004 Chemical tuning of metal–semiconductor interfaces *Phys. Rev. Lett.* **93** 136801
[7] Widdra W *et al* 2003 Time-resolved core level photoemission: surface photovoltage dynamics of the SiO_2/Si(1 0 0) interface *Surf. Sci.* **543** 87
[8] Pietzsch A, Föhlisch A, Hennies F, Vijayalakshmi S and Wurth W 2007 Interface photovoltage dynamics at the buried BaF_2/Si interface: time resolved laser-pump/synchrotron-probe photoemission *Appl. Phys. A: Mater. Sci. Process.* **88** 587
[9] Murdick R A, Raman R K, Murooka Y and Ruan C-Y 2008 Photovoltage dynamics of the hydroxylated Si(111) surface investigated by ultrafast electron diffraction *Phys. Rev.* B **77** 245329
[10] Schmuttenmaer C A, Aeschlimann M, Elsayed-Ali H E, Miller R J D, Mantell D A, Cao J and Gao Y 1994 Time-resolved two-photon photoemission from Cu(100): energy dependence of electron relaxation *Phys. Rev.* B **50** 8957
[11] Petek H and Ogawa S 1997 Femtosecond time-resolved two-photon photoemission studies of electron dynamics in metals *Prog. Surf. Sci.* **56** 239
[12] Knoesel E, Hotzel A and Wolf M 1998 Ultrafast dynamics of hot electrons and holes in copper: excitation, energy relaxation and transport effects *Phys. Rev.* B **57** 12812
[13] Cao J, Gao Y, Elsayed-Ali H E, Miller R J D and Mantell D A 1998 Femtosecond photoemission study of ultrafast electron dynamics in single-crystal Au(111) films *Phys. Rev.* B **58** 10948
[14] Weinelt M 2002 Time-resolved two-photon photoemission from metal surfaces *J. Phys.: Condens. Matter* **14** R1099
[15] Merschdorf M, Kennerknecht C and Pfeiffer W 2004 Collective and single-particle dynamics in time-resolved two-photon photoemission *Phys. Rev.* B **70** 193401
[16] Mathias S, Ruffing A, Deicke F, Wiesenmayer M, Aeschlimann M and Bauer M 2010 Band structure dependence of hot-electron lifetimes in a Pb/Cu(111) quantum-well system *Phys. Rev.* B **81** 155429
[17] Rhie H-S, Dürr H A and Eberhardt W 2003 Femtosecond electron and spin dynamics in Ni/W(110) films *Phys. Rev. Lett.* **90** 247201
[18] Lisowski M, Loukakos P A, Bovensiepen U, Staehler J, Gahl C and Wolf M 2004 Ultra-fast dynamics of electron thermalization, cooling and transport effects in Ru(001) *Appl. Phys.* A **78** 165
[19] Perfetti L, Loukakos P A, Lisowski M, Bovensiepen U, Berger H, Biermann S, Cornaglia P S, Georges A and Wolf M 2006 Time evolution of the electronic structure of 1T-TaS_2 through the insulator-metal transition *Phys. Rev. Lett.* **97** 067402
[20] Perfetti L, Loukakos P A, Lisowski M, Bovensiepen U, Eisaki H and Wolf M 2007 Ultrafast electron relaxation in superconducting $Bi_2Sr_2CaCu_2O_{8+\delta}$ by time-resolved photoelectron spectroscopy *Phys. Rev. Lett.* **99** 197001
[21] Schmitt F *et al* 2008 Transient electronic structure and melting of a charge density wave in $TbTe_3$ *Science* **321** 1649
[22] Rohwer T *et al* 2011 Collapse of long-range charge order tracked by time-resolved photoemission at high momenta *Nature* **471** 490
[23] Cortés R, Rettig L, Yoshida Y, Eisaki H, Wolf M and Bovensiepen U 2011 Momentum-resolved ultrafast electron dynamics in superconducting $Bi_2Sr_2CaCu_2O_{8+\delta}$ *Phys. Rev. Lett.* **107** 097002
[24] Aeschlimann M, Bauer M, Pawlik S, Knorren R, Bouzerar G and Bennemann K H 2000 Transport and dynamics of optically excited electrons in metals *Appl. Phys.* A **71** 485
[25] Lisowski M, Loukakos P A, Bovensiepen U and Wolf M 2004 Femtosecond dynamics and transport of optically excited electrons in epitaxial Cu films on Si(111)-7 × 7 *Appl. Phys.* A **79** 739
[26] Paggel J J, Miller T and Chiang T-C 1999 Quantum-well states as Fabry–Pérot modes in a thin-film electron interferometer *Science* **283** 1709
[27] Chiang T-C 2000 Photoemission studies of quantum well states in thin films *Surf. Sci. Rep.* **39** 181

[28] Milun M, Pervan P and Woodruff D P 2002 Quantum well structures in thin metal films: simple model physics in reality *Rep. Prog. Phys.* **65** 99
[29] Kirchmann P S, Rettig L, Zubizarreta X, Silkin V M, Chulkov E V and Bovensiepen U 2010 Quasiparticle lifetimes in metallic quantum-well nanostructures *Nat. Phys.* **6** 782
[30] Wei C M and Chou M Y 2002 Theory of quantum size effects in thin Pb(111) films *Phys. Rev.* B **66** 233408
[31] Zhang Y-F, Jia J-F, Han T-Z, Tang Z, Shen Q-T, Guo Y, Qiu Z Q and Xue Q-K 2005 Band structure and oscillatory electron–phonon coupling of Pb thin films determined by atomic-layer-resolved quantum-well states *Phys. Rev. Lett.* **95** 096802
[32] Hong I-P *et al* 2009 Decay mechanisms of excited electrons in quantum-well states of ultrathin Pb islands grown on Si(111): scanning tunneling spectroscopy and theory *Phys. Rev.* B **80** 081409
[33] Brun C, Hong I-P, Patthey F, Sklyadneva I Y, Heid R, Echenique P M, Bohnen K P, Chulkov E V and Schneider W-D 2009 Reduction of the superconducting gap of ultrathin Pb Islands grown on Si(111) *Phys. Rev. Lett.* **102** 207002
[34] Zhang T *et al* 2010 Superconductivity in one-atomic-layer metal films grown on Si(111) *Nat. Phys.* **6** 104
[35] Kirchmann P S, Wolf M, Dil J H, Horn K and Bovensiepen U 2007 Quantum size effects in Pb/Si(111) investigated by laser-induced photoemission *Phys. Rev.* B **76** 075406
[36] Dil J H, Kim J W, Kampen Th Horn K and Ettema A R H F 2006 Electron localization in metallic quantum wells: Pb versus in on Si(111) *Phys. Rev.* B **73** 161308
[37] Upton M H, Wei C M, Chou M Y, Miller T and Chiang T-C 2004 Thermal stability and electronic structure of atomically uniform Pb films on Si(111) *Phys. Rev. Lett.* **93** 026802
[38] Yeh V, Berbil-Bautista L, Wang C Z, Ho K M and Tringides M C 2000 Role of the metal/semiconductor interface in quantum size effects Pb/Si(111) *Phys. Rev. Lett.* **85** 5158
[39] Slomski B, Meier F, Osterwalder J J and Dil J H 2011 Controlling the effective mass of quantum well states in Pb/Si(111) by interface engineering *Phys. Rev.* B **83** 035409
[40] Kirchmann P S and Bovensiepen U 2008 Ultrafast electron dynamics in Pb/Si(111) investigated by two-photon photoemission *Phys. Rev.* B **78** 035437
[41] Kiss T, Shimojima T, Ishizaka K, Chainani A, Togashi T, Kanai T, Wang X-Y, Chen C-T, Watanabe S and Shin S 2008 A versatile system for ultrahigh resolution, low temperature and polarization dependent laser-angle-resolved photoemission spectroscopy *Rev. Sci. Instrum.* **79** 023106
[42] Doniach S and Sunjic M 1970 Many-electron singularity in X-ray photoemission and X-ray line spectra from metals *J. Phys. C: Solid State Phys.* **3** 285
[43] Fann W S, Storz R, Tom H W K and Bokor J 1992 Direct measurement of nonequilibrium electron-energy distributions in subpicosecond laser-heated gold films *Phys. Rev. Lett.* **68** 2834
[44] Anisimov S I, Kapeliovich B L and Perelman T L 1974 Electron emission from metal surfaces exposed to ultrashort laser pulses *Sov. Phys.—JETP-USSR* **39** 375
[45] Allen P B 1987 Theory of thermal relaxation of electrons in metals *Phys. Rev. Lett.* **59** 1460
[46] Del Fatti N, Voisin C, Achermann M, Tzortzakis S, Christofilos D and Vallée F 2000 Nonequilibrium electron dynamics in noble metals *Phys. Rev.* B **61** 16956
[47] Rethfeld B, Kaiser A, Vicanek M and Simon G 2002 Ultrafast dynamics of nonequilibrium electrons in metals under femtosecond laser irradiation *Phys. Rev.* B **65** 214303
[48] Luh D-A, Miller T, Paggel J J and Chiang T-C 2002 Large electron–phonon coupling at an interface *Phys. Rev. Lett.* **88** 256802
[49] Smith N V 1985 Phase analysis of image states and surface states associated with nearly-free-electron band gaps *Phys. Rev.* B **32** 3549
[50] Dekorsy T, Cho G C and Kurz H 2000 *Coherent Phonons in Condensed Media Springer Topics in Applied Physics* vol 76 (Berlin: Springer)
[51] Hase M, Ishioka K, Demsar J, Ushida K and Kitajima M 2005 Ultrafast dynamics of coherent optical phonons and nonequilibrium electrons in transition metals *Phys. Rev.* B **71** 184301
[52] Hase M and Kitajima M 2010 Interaction of coherent phonons with defects and elementary excitations *J. Phys.: Condens. Matter* **22** 073201

[53] Ishioka K and Misochko O V 2010 Coherent lattice oscillations in solids and their optical control *Progress in Ultrafast Intense Laser Science (Springer Series in Chemical Physics* vol 98*)* ed K Yamanouchi, A Giulietti, K Ledingham, F P Schäfer, J P Toennies and W Zinth (Berlin: Springer) pp 23–63

[54] Landolt Boernstein 1976 *Numerical Data and Functional Relationships in Science and Technology New Series* (Berlin: Springer)

[55] Rowell J M, Mcmillan W L and Feldmann W L 1969 Phonon spectra in Pb and $Pb_{40}Tl_{60}$ determined by tunneling and neutron scattering *Phys. Rev.* **178** 897

[56] Savrasov S Y and Savrasov D Y 1996 Electron–phonon interactions and related physical properties of metals from linear-response theory *Phys. Rev.* B **54** 16487

[57] Yndurain F and Jigato M P 2008 First principles calculation of localized surface phonons and electron–phonon interaction at Pb(111) thin films *Phys. Rev. Lett.* **100** 205501

[58] Braun J, Ruggerone P, Zhang G, Toennies J P and Benedek G 2009 Surface phonon dispersion curves of thin Pb films on Cu(111) *Phys. Rev.* B **79** 205423

[59] Bovensiepen U 2007 Coherent and incoherent excitations of the Gd(0001) surface on ultrafast timescales *J. Phys.: Condens. Matter* **19** 083201

[60] Melnikov A, Radu I, Bovensiepen U, Krupin O, Starke K, Matthias E and Wolf M 2003 Coherent optical phonons and parametrically coupled magnons induced by femtosecond laser excitation of the Gd(0001) surface *Phys. Rev. Lett.* **91** 227403

[61] Dil J H, Kim J W, Gokhale S, Tallarida M and Horn K 2004 Self-organization of Pb thin films on Cu(111) induced by quantum size effects *Phys. Rev.* B **70** 045405

[62] Dil J H, Kampen T U, Hülsen B, Seyller T and Horn K 2007 Quantum size effects in quasi-free-standing Pb layers *Phys. Rev.* B **75** 161401